STATUS AND OUTLOOK OF FUSION RESEARCH

Wolfgang Biel[a,b]

[a]*Institute of Energy and Climate Research, Forschungszentrum Jülich GmbH, D-52425 Jülich, Germany*

[b]*Department of Applied Physics, Ghent University, B-9000 Ghent, Belgium*

ABSTRACT

Fusion research aims to develop fusion as a promising energy source for the future. The latest status of fusion research is represented in the physics and technology basis of the large tokamak ITER [1] currently under construction, which is expected to produce for the first time significant fusion power (P_{fus} ~ 500 MW) over periods of several minutes. After a successful operation of ITER, several countries are planning the development of demonstration reactors with net electricity production to prepare the ground for commercialisation. While the main mission of ITER is the demonstration of a hot plasma mainly heated by fusion alpha particles, future efforts must be targeted towards improving the performance and availability of the reactor, and demonstrating the economic perspective for commercial fusion energy.

Within this paper we present an overview on the status of fusion and on our current understanding of the main features of a tokamak fusion reactor. Aiming for a quantitative treatment, a coupled set of non-linear equations is used to describe and predict the reactor performance based on a limited set of input quantities in a self-consistent way (systems code approach). Operational limits related to both plasma operation and machine components are discussed and an optimisation strategy to define the various plasma and machine parameters is outlined.

I. INTRODUCTION

The controlled fusion of the hydrogen isotopes deuterium (D) and tritium (T) has a great potential to provide substantial contributions to the energy supply of mankind for the future. Fusion research is on the one hand aiming to improve our basic understanding of fusion plasmas and of the principles of confining and controlling them, and on the other hand a targeted approach is pursued to develop the first fusion power plant which will be feeding electrical energy into the grid. Specifically, the European Roadmap for Fusion [2] is providing a plan on how to conduct the development of a demonstration reactor (DEMO), aiming for a net electricity production of 300…500 MW by the mid of this century. In this plan, the development and successful operation of the ITER tokamak [1] is seen as a cornerstone.

ITER is supposed to produce for the first time plasma pulses with a significant fusion power P_{fus} = 500 MW at an energy amplification factor of $Q = P_{fus}/P_{ext}$ = 10 over a pulse duration of t_{pulse} = 400 s, where P_{ext} denotes the externally supplied plasma heating power. Due to the size and the complexity of the ITER project which is currently under development in Cadarache, France, these decisive results can realistically be expected only after 2030.

The mission of ITER is focussed towards the physics of a fusion plasma which is predominantly heated by the alpha particles generated via fusion, and to a demonstration of several reactor relevant technologies. The target value of Q = 10 would however not yet be suitable for efficient net electricity production, since the external plasma heating consumes electrical power, and therefore

$$(1) \qquad P_{el,net} \sim \eta_{el} P_{therm} - \frac{P_{ext}}{\eta_{ext}} \sim P_{therm}\left(\eta_{el} - \frac{1}{\eta_{ext} Q}\right).$$

In case of a thermodynamic efficiency for conversion of thermal power to electricity of η_{el} ~ 0.3, and for a typical efficiency for the production of the external plasma heating power from electrical power of η_{ext} ~ 0.3 [3], a value of Q = 10 represents just the "break-even" above which net electricity production would become possible. Thus, in order to produce net electricity, DEMO will have to obtain an energy amplification factor of $Q >> 10$, where the exact value is however not important and is hence not regarded as an optimisation quantity.

Considering the timescale of the ITER project as well as the budgetary limitations, the remaining period until the year ~ 2050 for achieving DEMO operation with electricity production appears quite short. Hence this ambitious goal can only be achieved if many of the main physics and technology developments for ITER can be smoothly transferred towards DEMO, such that only a limited amount of major new developments will be needed after ITER. In this respect the tokamak concept, together with the ITER developments, is the most developed magnetic confinement concept, and it has therefore been adopted as the "baseline" for a DEMO fusion reactor in the European Roadmap. In the following, we describe some aspects of the tokamak as needed for the systems description of the reactor. For a more detailed description of the tokamak principle and the status of related research we refer to the textbook by Wesson [4].

II. PHYSICS PRINCIPLES RELEVANT TO THE DESIGN OF A TOKAMAK FUSION REACTOR

A. Basics of fusion

A thermal pure DT plasma with a D-T ratio of 50:50, where the alpha particle power is compensating the power losses from the plasma, can be sustained ("ignited plasma") if the burn condition is fulfilled [4]

$$(2) \quad n_{DT}\, k_B T_i \tau_E > 3 \cdot 10^{21}\,\mathrm{keV \cdot s \cdot m^{-3}}.$$

Here n_{DT} denotes the density of deuterium and tritium ions, k_B is the Boltzmann constant, T_i the ion temperature and

$$(3) \quad \tau_E = \frac{W_{plasma}}{P_{heat}}$$

is the global energy confinement time, with W_{plasma} being the stored kinetic energy in the plasma and P_{heat} the heating power absorbed in the plasma. Hence the energy confinement time is a measure of the quality of the thermal insulation of the plasma.

A minimum value of the triple product needed for ignition is found in the range of T_i = 10 … 20 keV. Assuming this temperature range and a fuel ion density of $n_{DT} \sim 10^{20}$ m^{-3}, the burn condition can be fulfilled if the energy confinement time amounts $\tau_E \sim$ several seconds.

The fusion power density produced in a thermal DT plasma with D-T ratio 50:50 follows from the equation

$$(4) \quad \frac{P_F}{V} = \frac{1}{4} n_{DT}^2 < \sigma v >_{DT} E_{DT},$$

where $<\sigma v>$ denotes the rate coefficient for the DT fusion reaction, see fig. 1, and E_{DT} = 17.59 MeV is the energy released per fusion event. A functional expression for the fusion rates was presented by Bosch et al. [5].

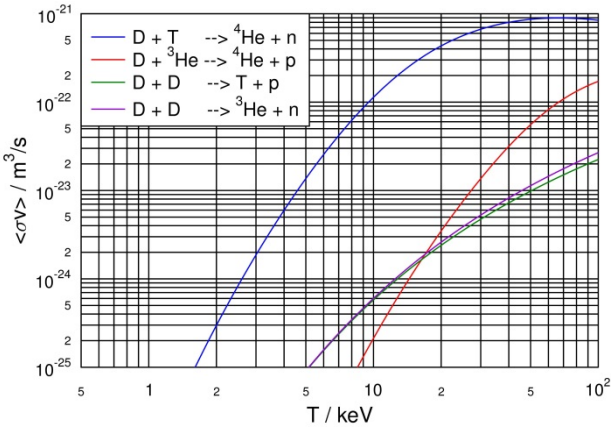

Figure 1: Fusion rate coefficients after Bosch et al. [5]

In the presence of plasma impurities with charge state Z,

$$(5) \quad n_{DT} = n_e - \sum Z\, n_Z := f_{nDT}\, n_e,$$

where n_Z denotes the density of ion species Z and the summation comprises all ion species apart from deuterium and tritium.

B. The tokamak principle

The most widely used principle to confine a hot fusion plasma in a magnetic field is the tokamak, a toroidal plasma confinement system. In a tokamak, toroidal field (TF) coils generate a strong toroidal magnetic field, forcing the charged particles in the plasma to gyrate along the field lines. A purely toroidal field would however lead to a loss of the plasma particles into radial outward direction via particle drifts, originating from the curvature and inhomogeneity of the field. These losses can be suppressed by adding a poloidal field (PF) component.

In the tokamak the poloidal field is generated by driving a current in the plasma, using the central solenoid (CS) coil as the primary and the plasma as the secondary winding of a transformer. The helical magnetic field resulting from the superposition of TF and PF field components has a field line structure in the form of nested magnetic surfaces – in the absence of radial motion any particle following its field line would stay on its magnetic surface. A vertical magnetic field, which is generated by poloidal field coils, interacts with the plasma current to provide a radially inward $j \times B$ force to counteract the Lorentz and pressure forces acting in radial outward direction, thereby keeping the diameter of the plasma torus constant.

The geometry of the basic tokamak plasma is described by the major radius R_0 and minor radius a of the torus, as well as the safety factor q. This safety factor measures the number of toroidal turns which are needed until a screwed field line would come back to the same poloidal position. The outer boundary of the plasma (minor plasma radius a) in a tokamak can be defined by two different ways.

In a simple tokamak, the most protruding wall element, the so called "limiter", will cut a magnetic field line, thus defining the outermost magnetic surface: all magnetic field lines inside of this surface are closed, while all field lines outside are open and are ending on the wall elements. The limiter is the area where most of the plasma wall interaction and heat exhaust takes place. The impinging particles are being neutralised, and the continuous plasma flux towards the limiter causes some neutral particle compression in front of it. This effect can be used to pump away impurities like the helium ash from the plasma of a fusion reactor. Usually a limiter is constructed from a material with high melting point and good thermal conductivity, together with a smooth surface shaping, in order to withstand the very high heat loads in the plasma wall contact.

However, in most modern tokamaks large poloidal field coils are employed to elongate the plasma in vertical direction, generating „X-points" at the locations where the poloidal fields of the plasma current and of the

PF coil just cancel. Thus the strongest (innermost) X-point defines the "separatrix" which divides the magnetic field lines into two categories: Inside the separatrix, all field lines are closed and they lie on nested magnetic surfaces. Outside the separatrix, all magnetic field lines are open and they impinge, eventually after several toroidal turns, onto a wall element within the so called "divertor" which is usually located below the main plasma. If the distance between first wall of the main chamber and plasma edge is chosen large enough, the particles lost from the main plasma in radial direction may not touch the first wall but stream along the field lines down towards the divertor. On their way they cool down via radiation and collisions and finally form a relatively cold plasma of high density ("divertor plasma") in front of the divertor target plates. This concept was designed to separate the plasma wall interaction zone from the core plasma, to make the heat loads to the first wall more tolerable than in a limiter tokamak, and to facilitate the Helium pumping by the neutral particle compression arising from the plasma flow towards the target plates followed by neutralisation. In most cases only one main divertor is used in a so called "single null" configuration, where the plasma geometry can be described by the two new parameters elongation κ and triangularity δ in addition to the major and minor radius.

For the following discussion of the main dependencies of fusion power in a divertor tokamak, it is convenient to write all equations in terms of dimensionless quantities:

a	Minor plasma radius at the tokamak midplane / m
R_0	Major plasma radius at the tokamak midplane / m
n_{20}	Electron density / 10^{20} m^{-3}
n_{DT}	Fuel ion density / 10^{20} m^{-3}
n_Z	Density of ions with charge state Z / 10^{20} m^{-3}
N_{GW}	Greenwald number $N_{GW} = n/n_{GW}$
T_k	Plasma temperature / keV
I_M	Plasma current / MA
B_0	Magnetic field at the tokamak axis $R = R_0$ / T
q_{95}	Safety factor at a radial location of 95% flux
P_M	Power / MW
W	Energy / MJ
V	Plasma volume / m^3
τ_E	Energy confinement time / s

C. High confinement regime (H-mode)

An important feature of divertor tokamaks is the occurrence of improved plasma confinement in case of sufficiently strong plasma heating. In this so called "H-mode" [6] the observed energy confinement time τ_E can be a factor ~ 2 higher than in the low confinement ("L-mode") regime. The H-mode is related to the formation of a transport barrier and a "pedestal" of the pressure at the plasma edge. The properties of the H-mode have been widely investigated on many divertor tokamaks, deriving the empirical IPB98(y,2) scaling law by a nonlinear fitting procedure using data from a large number of discharges [7]:

$$(6) \quad \tau_E = 0.173\, H_H I_M^{0.93} R_0^{1.39} a^{0.58} \kappa^{0.78} n_{20}^{0.41} B_0^{0.15} P_{loss,M}^{-0.69} .$$

In eq. (6) the confinement enhancement factor H_H is a measure of the actual confinement quality relative to standard H-mode (H_H = 1.0), and we have eliminated the dependency on the isotope composition by assuming a DT plasma with $n_D = n_T$.

In order to achieve and maintain H-mode conditions, the power losses $P_{loss} = P_{heat} - P_{rad,core}$ across the separatrix via convection and conduction have to exceed the H-mode power threshold P_{LH} ($P_{rad,core}$ denotes the radiated power from the core plasma). Within this paper, we use the empirical scaling presented by Martin et al. [8]

$$(7) \quad P_{LH,M} = 1.72\, n_{20}^{0.78} B_0^{0.77} a^{0.98} R_0^{1.00} .$$

D. Operational limits in a tokamak plasma

In order to maximise the fusion power density according to eq. (4), both the plasma density and temperature should be maximised. However, the parameter range in which the plasma in a tokamak fusion reactor can be operated is governed by several operational limits which are only briefly recalled here. For a more detailed treatment, we refer to the literature [4, 9].

First, the line averaged plasma density is limited by the empirical "Greenwald limit" [10]:

$$(8) \quad n_{20} \le n_{GW} = \frac{I_M}{\pi a^2} .$$

Increasing the plasma density to values above n_{GW} leads to a termination (disruption) of the discharge by an instability. Stable tokamak operation can only be obtained if, for a desired plasma density, the plasma current is large enough or the plasma radius small enough. However, the plasma current within a divertor tokamak is limited via a second requirement, such that the safety factor q_{95} (number of toroidal turns after which a magnetic field line closes with one poloidal turn) measured at a radial location of 95% flux must stay above a value of 2 in order to avoid a disruption caused by an external kink mode [11]

$$(9) \quad q_{95} = 5 \frac{a^2 B_0}{I_M R_0} f \ \ge 2 ,$$

where we have used the geometric shape factor [7]

$$(10) \quad f = \frac{1+\kappa^2\left(1+2\delta^2-1.2\delta^3\right)}{2} \, \frac{1.17-0.65\, a/R_0}{\left(1-(a/R_0)^2\right)^2} .$$

From eqs. (9) and (10) it is evident that choosing larger elongation and triangularity would increase the shape factor *f* and hence open a route to allow for larger plasma current and hence higher density. The vertical elongation κ and the triangularity δ of the plasma are defined by the equilibrium between the plasma pressure and the action of the poloidal field coils onto the plasma. However, increasing the elongation by enhancing the attractive forces induced by the PF coils located above and below the plasma would make the vertical plasma position more and more unstable. In order to control the vertical position, the response of the control system must be faster than the growth rate of the vertical instability. The limiting factors here are first the large inductivity of the PF coils, second the limitations for both the maximum voltage and maximum power to be supplied to the coils, and third the damping by eddy currents induced in the blanket and structures between PF coils and plasma. Based on these boundary conditions the plasma elongation has to be limited towards a value that can be safely controlled. According to experimental and modelling results, for DEMO a maximum controllable elongation at the X-point of

$$(11)\quad \kappa_{x,\max} = 1.5 + \frac{0.5}{A-1}$$

has been proposed [12], where $A = R_0/a$ is the aspect ratio of the plasma. Following eq. (9), another route to attain higher plasma current and hence higher plasma density would be opened by increasing the magnetic field B_0 or reducing the major radius R_0 while keeping the minor radius constant.

As a third requirement, the plasma pressure in a tokamak is limited by the "Troyon limit" [4]

$$(12)\quad \beta_N \equiv 100\,\beta \Big/ \frac{I_M}{a\,B_0} \le \beta_{N,\max},$$

where

$$(13)\quad \beta \equiv \frac{p}{B_0^2/2\mu_0}$$

is the normalised plasma pressure ("beta"). For discharges of the "ELMy H-mode" type the empirical limitation for the normalised beta is $\beta_{N,max} = 3.5$. In case of a reactor design based on "conservative" physics and technology assumptions as discussed below, the expected beta is low enough so that the beta limit will not be further discussed in the following.

E. Systems description of a tokamak reactor

In the following, we present a simple quantitative description of the main elements of a tokamak fusion reactor. Writing for the kinetic plasma energy

$$(14)\quad W_{plasma} \sim 3\,n\,k_B\,T\,V_{plasma},$$

assuming $T_e = T_i = T$, neglecting the radial dependencies of both *n* and *T*, and inserting into eq. (3), we obtain

$$(15)\quad T_k = 1.05\,\frac{\tau_E\left(P_{\alpha,M} + P_{ext,M}\right)}{\kappa\,a^2\,R_0\,n_{20}}.$$

Here, we have assumed that the total heating power is given by the sum of alpha heating power and external heating power, $P_{heat} = P_\alpha + P_{ext}$, and we have approximated the core plasma volume by the expression

$$(16)\quad V_{plasma} \sim 2\pi^2\kappa a^2 R_0.$$

The system of equations (4), (6) and (15) already allows to perform a 0-D description of the tokamak fusion reactor and to predict the expected fusion power output for a given set of pre-defined input parameters, namely the plasma geometry (a, R_0, κ and δ), plasma density, magnetic field B_0, plasma current (safety factor) and confinement quality H_H. This procedure, together with a treatment of plasma radiation (see below) also represents the essence of the plasma physics module in more sophisticated so called "fusion reactor systems codes" [13,14,15,16]. For simplicity we will use in the following discussion radially constant (mean) values for plasma density and temperature. However, extending the description towards using prescribed radial profiles is straightforward and this is the usual approach by systems codes.

For a discussion on the principles for optimisation of a fusion reactor, this set of equations is somewhat involved and hence impractical. We therefore proceed with simplifying the description further by restricting the discussion to cases where the plasma temperature is in the range of $T = 10 \ldots 20$ keV, where the rate coefficient shows approximately a quadratic dependence with plasma temperature and hence

$$(17)\quad \begin{aligned} P_\alpha &= V_{Plasma}\,n_D n_T \left\langle \sigma v \right\rangle_{DT} \times \frac{17.59}{5} MeV \\ &\sim 0.0016\,n_{20}^2\,T_k^2\,V_{Plasma}\,[MW] \end{aligned}.$$

Furthermore, it is convenient to substitute plasma current and density in the expressions for confinement time (6) and plasma temperature (15) by the expressions for the dimensionless quantities q_{95} and $N_{GW} = n/n_{GW}$, yielding

$$(18)\quad \tau_E = 0.935\,H_H\,R_0^{0.05}\,a^{2.44}\,\kappa^{0.78}\,f^{1.34}\,N_{GW}^{0.41}\,q_{95}^{-1.34}\,B_0^{1.49}\,P_M^{-0.69}$$

and

$$(19)\quad \begin{aligned} T_k = 0.62\,H_H\,R_0^{0.05} a^{0.44} \kappa^{-0.22} f^{0.34} \times \\ N_{GW}^{-0.59} q_{95}^{-0.34} B_0^{0.49} \left(P_{\alpha,M} + P_{ext,M}\right)^{0.31}. \end{aligned}$$

Neglecting for the moment the radiated power and the heating power, i.e. assuming $P_{heat} = P_{loss} = P_\alpha$, we obtain after some algebra a single equation describing the alpha heating power generated in a tokamak fusion reactor operated at H-mode ("tokamak fusion reactor equation")

$$(20)\quad P_{\alpha,M} = 10^{-4}\,H_H^{5.26} a^{7.58} R_0^{-2.37} \kappa^{1.47} f^{7.05} N_{GW}^{2.16} q_{95}^{-7.05} B_0^{7.84}$$

In this equation, the dimensionless formulations of the density limit and the current limit

(21) $N_{GW} \leq 1$ and

(22) $q_{95} \geq 2$

have to be observed. For the geometrical parameters of the tokamak used in eq. (20), the following condition applies:

(23) $R_0 > a + b + c + r_{CS}$,

where c denotes the radial thickness of the TF coil and r_{CS} the radius of the central solenoid.

Using N_{GW}, the beta limit ($\beta_N < 3.5$) can be reformulated as

(24) $T_k \leq 1.35\ B_0\ a / N_{GW}$.

After solving the equations above for a set of input parameters, the resulting temperature T_k (eq. 15) should be in agreement with condition (24) to avoid the pressure driven instabilities leading to a plasma disruption.

In a reactor under steady state conditions all the power which is heating the core plasma has to be exhausted from the plasma, without damaging the wall or divertor. We express the power entering into the divertor via

(25) $P_{Div} \approx P_{loss} \approx P_\alpha + P_{ext} - P_{rad,core}$.

Practically, the radiated power $P_{rad,core}$ in the core plasma can be adjusted in a wide range by adding medium- or high-Z impurities like Argon, Krypton or even Xenon to the plasma [17]. A simple empirical expression for the total radiated power from a tokamak plasma was presented by Matthews et al. [18],

(26) $P_{rad} \approx 0.16 \left(Z_{eff} - 1\right) S^{0.94}\ n_{20}^{1.9} \quad [MW]$,

where S denotes the surface area of the plasma. However, the power loss across the separatrix has to significantly exceed the H-mode threshold (eq. 7) in order to avoid a sudden drop of confinement back to low confinement (L-mode) conditions. Furthermore, the radiation loss parameter L_Z, which is defined via the relation

(27) $P_{rad,Z} = n_Z n_e L_Z$,

typically shows an increase with decreasing electron temperature over a wide range of temperatures, which implies that highly radiative plasmas are difficult to control: any sudden drop of confinement and plasma temperature would lead to an increase of radiation and hence to a further cooling of the plasma. This is not reflected in the eq. (26), which hence only can serve as a rough approximation for the radiated power.

Within the divertor region, a large fraction of P_{Div} still has to be radiated in order to distribute the power to larger parts of the target plates and hence keep the peak loads below the tolerable values.

In addition to the output power of a tokamak fusion reactor, a second important optimisation quantity is the plasma pulse duration which can be achieved. This pulse duration depends on the plasma current, the ohmic resistance and plasma inductivity, the amount of non-inductive current driven by the external heating [3] or by the "bootstrap" effect [4], and on the available total flux swing [19]. The total flux Φ_0 available from the central solenoid (CS) and (to some extent) from the other poloidal field (PF) coils,

(28) $\Phi_0 \approx 1.1 \times 2\pi r_{CS}^2\ B_{\max,CS}$,

where $B_{max,CS}$ denotes the maximum magnetic field obtained in the CS coil and the factor 1.1 accounts for a conservative estimate of the additional flux provided by the PF coils. During the plasma discharge, this total flux is consumed by the ignition $\Phi_{ignit.}$, by the build-up of the magnetic energy stored in the plasma current, and by ohmic losses. After having tuned the CS coil from $B_{max,CS}$ towards the final value of $-B_{max,CS}$, the plasma current has to be ramped down and the discharge has to be stopped. Approximating the ohmic losses during current ramp-up using the Ejima approximation $\Phi_{OH,ramp-up.} \sim 0.5 \mu_0 R_0 I_P$ [20], we obtain for the pulse duration

(29) $t_{pulse} \approx \dfrac{\Phi_0 - \Phi_{ignit.} - \left(0.5\mu_0 R_0 + L_{plasma}\right) I_P}{R_{plasma}\left(I_P - I_{noninduct}\right)}$,

where R_{plasma} denotes the ohmic resistance of the plasma during the flat-top period, and $I_{noninduct}$ is the non-inductive part of the total plasma current. According to eq. (29), long pulse operation can be attained by increasing Φ_0 or by enhancing the non-inductive current. In case of full noninductive current drive ($I_{noninduct} = I_P$), which is the domain of "advanced tokamak" studies [21], steady state operation is obtained, where usually high confinement quality $H_H > 1.0$ is assumed, allowing for higher plasma pressure and hence larger bootstrap current, while lower values for the total plasma current are chosen with $q_{95} = 4 \ldots 6$ in order to keep the level of the required external current drive within reasonable limits.

III. TECHNOLOGICAL ISSUES RELEVANT TO REACTOR OPTIMISATION

Before continuing the discussion of eq. (20) and the reactor optimisation strategy, we briefly recall a number of technological issues relevant to the definition of reactor parameters.

A. Magnetic field coils

From Eq. (20) it can be seen that the fusion power depends strongly on the toroidal magnetic field B_0 in the plasma centre, if the safety factor q_{95}, the Greenwald fraction N_{GW}, the confinement quality H_H and the plasma geometry as defined by the four parameters R_0, a, κ and δ are kept constant. The latest status of superconducting magnet coil technology for fusion is

represented by the development of the ITER coils [22]. Two important limitations have to be observed for the TF coils design. First, the current density in the superconducting materials at a given temperature and magnetic field must be kept below a limit to avoid back-transition to normal conductivity. Thus the size of the winding pack of the TF coils is defined by these requirements together with Biot-Savart's law describing the required Amp-turns

$$(30)\quad B_{tor}(R) = \frac{\mu_0}{2\pi}\frac{N\,I}{R},$$

where N is the total number of windings (product of number of coils and number of windings per coil), I is the current per winding and R the distance from the torus centre. Second, the coils are subject to the "hoop" force which acts to expand each conductor and the TF coil as a whole, and a strong radial force driving all conductors away from the plasma centre. Both forces have to be supported by the coil design. For this purpose, the cable in conduit approach has been adopted for ITER. Here the individual brittle SC conductors ("strands") are packed together with Copper strands, needed in cases of quench of the superconductive state, into stainless steel housings to form a robust cable structure which supports the whole set of strands against the forces. These SC cables are then wound into radial plates which are designed to accept the overall forces acting on the cables. The radial plates itself are mounted into a thick steel casing taking the overall forces acting onto the coil. The ITER TF coil structure, with a radial coil thickness in the order of $c \sim 1$ m and with a maximum field at the inner leg of the TF coil of $B_{max} = 11.6$ T, is subject to stresses of up to 600 MPa, which is near the limits of the steel that is used here. Aiming for even higher toroidal magnetic fields would imply

- increasing the number of Amp-turns according to eq. (30), which means increasing the area needed for the winding pack;
- on the same time, strongly reducing the current density in the SC strands, since the permissible current density in the SC conductor decreases with magnetic field, which means another increase in the area of the winding pack;
- finally, increasing the amount of steel in the radial plates and coil housings to accept the stronger forces.

From all three effects together it follows that, in order to obtain higher magnetic field B_{max}, the radial dimension of the TF coils c would have to be enlarged proportional to a high power of the magnetic field. Practically, from the current status of magnet technology for fusion, the values of $B_{max,TF} = 11.6$ T and $B_{max,CS} = 13$ T achieved for the ITER design are regarded as a technical limitation, which also defines the framework for the DEMO design studies undertaken in Europe [23].

B. Blanket design

While ITER can be operated using tritium that is available on earth, e.g. produced as a side product from fission plants, the tritium consumption of a DEMO reactor will be so large (several 10 kg per year) that the tritium will have to be produced on-site by a breeding process using the fusion neutrons. For this purpose, the plasma of a DEMO reactor will be almost completely surrounded by a breeding blanket, where Lithium is being converted to tritium using the reactions

$$(31)\quad \begin{array}{l} {}^{6}Li + n \rightarrow T + \alpha + 4.78MeV \\ {}^{7}Li + n \rightarrow T + \alpha + n - 2.47MeV \end{array}.$$

Natural Lithium consists of 7.4% ^{6}Li and 92.6% ^{7}Li, but the cross section for the first (exothermic) reaction is more than two orders of magnitude larger for the case of thermalized neutrons, as compared to the peak of the cross section for the second (endothermic) reaction. A pure breeding blanket cannot obtain a tritium breeding rate (TBR, ratio between produced and consumed tritium) of 100 percent, since a fraction of the primary fusion neutrons will unavoidably be lost due to absorption in the structural material of the blanket, and due to geometrical neutron losses related to the necessary openings for plasma diagnostic, heating and fuelling systems, as well as within the divertor [24]. Therefore the overall number of available neutrons has to be increased by a neutron multiplication process. For this purpose, the following reactions are being considered:

$$(32)\quad \begin{array}{l} {}^{9}Be + n \rightarrow 2\,{}^{4}He + 2n - 2.5MeV \\ {}^{208}Pb + n \rightarrow {}^{207}Pb + 2n - 7.4MeV \end{array}$$

In addition to the generation of neutrons, another main function of the blanket is the power exhaust in a way that permits the efficient use of the thermal power to produce electrical energy.

For the design of the blanket, various technical implementations and different options are under development. If Beryllium is used as multiplier, both the Lithium breeder and the Beryllium are commonly foreseen in the form of small solid pebbles within the blanket module. Designs based on Lead as multiplier are normally based on mixing both breeder and multiplier and operating the Pb:Li mixture at temperatures of several hundred degrees as a liquid metal. Regarding the choice of coolants, various options are being considered, namely water cooling, Helium gas cooling and (in case of Pb:Li) the liquid metal itself, as well as dual-coolant options using the combination of water and Helium, or liquid metal and water. Helium as coolant could provide higher exit temperatures than water and hence allow for higher thermodynamic efficiency, but the large amounts of gas needed for cooling require significant pumping power, which largely reduces the overall efficiency again. In addition to the TBR and the overall thermodynamic efficiency also the thickness of the blanket is an important optimisation criterion for the

reactor: The distance b between plasma and TF coil on the inboard side of the tokamak is related to the magnetic field in the plasma, B_0, and the field B_{max} at the inner leg of the TF coil according to Biot-Savart's law via

$$B_0 = B_{\max}\left(1 - \frac{a+b}{R_0}\right). \quad (33)$$

Hence reducing b would allow for larger magnetic field in the plasma B_0, leading to an increase of fusion power when keeping all other quantities constant. However, the quantity b is defined as the sum of several radial dimensions:

- the radial distance needed between plasma edge and first wall in order to protect the first wall from overheating,
- the thickness of the breeding blanket, including the space needed for the cooling manifold at the backside of the blanket,
- shielding and vacuum vessel thickness.

In a tokamak reactor with full tritium breeding the total distance between the inner radial edge of the plasma and the inner leg of the TF coil cannot be made significantly smaller than $b \sim 1.8$ m. Since this is a quantity essentially not scaling with the size of a fusion reactor, the quantity b represents a lower limitation for the overall radial dimensions of the reactor.

In the European programme towards a DEMO reactor, the Helium Cooled Pebble Bed (HCPB) and the Helium Cooled Lithium lead (HCLL) concepts being are pursued as the main concepts, while the Dual Coolant Lithium Lead (DCLL) and the Water Cooled Lithium Lead (WCLL) designs are regarded as alternative approaches [25].

C. First wall and divertor

The first wall in the main chamber of a DEMO fusion reactor has to withstand a typical level of average stationary surface heat loads due to radiated power and particles emitted from the core plasma in the order of less than 0.5 MW/m^2, where some local inhomogeneities due to the magnetic field and wall structure have to be expected. On top of this a typical stationary neutron wall load in the order of 1-2 MW/m^2 provides the main part of the power produced from the fusion processes, which is mainly deposited into the first 10-30 cm of the blanket. The stationary heat loads at the first wall can reasonably be covered by installing a sufficiently dense (mm … cm) network of coolant channels into the involved components. In this area, a low activation steel like EUROFER is foreseen as structural material.

Strong transient heat loads to the first wall can be generated by plasma disruptions and they are a major area of concern already for ITER [26]. During a plasma disruption, the confining nested magnetic field structure breaks down due to rapid changes in the plasma current and current profile, which leads to a rapid loss of a major part of the stored kinetic energy to the wall ("thermal quench") within a short time of the order of $\tau_{TQ} \leq 1$ ms. The main strategy for ITER, besides avoidance of disruptions, is the disruption mitigation via fast and massive particle injection into the plasma once a disruption can no longer be avoided. The injected particles get excited and radiate major fractions of the stored energy, thereby distributing the heat loads to larger areas. Assuming that half of the stored thermal energy from the DEMO plasma $W_{th} \sim 1$ GJ would be radiated to the first wall within a time of $\tau_{TQ} \sim 1$ ms, and assuming a toroidal and poloidal asymmetry of a factor 2 each, the resulting maximum heat impact factor η [27] on DEMO is in the order of

$$\eta = \frac{W}{A_{eff}\sqrt{\tau_{TQ}}} \sim 40\frac{MJ}{m^2 s^{0.5}} \quad (34)$$

(W is the deposited energy, A_{eff} the effective wall area), which is only slightly below the melt limit for tungsten but already above the limit where surface cracks of several 100 microns depth have to be expected. Thus only a low number of disruptions is permissible on DEMO even with application of a perfect mitigation system.

The divertor target plates have to withstand the highly peaked stationary power fluxes that are transporting the power, which has been convected and conducted across the separatrix, along the field lines down to the divertor region. The peak power flux densities expected for ITER are in the order of 10…20 MW/m^2. To accommodate for these extreme heat loads, the divertor target plates of ITER are constructed using a castellated tungsten surface connected to a Cu:Cr:Zr alloy structure, where a dense network of cooling channels serves for heat removal using water at 100 °C as coolant.

For a future DEMO reactor, staying above the H-mode threshold (eq. 7) implies that the expected stationary peak power flux densities are comparable or even larger than on ITER. On the other hand, several routes of modifications are being pursued to develop the DEMO divertor aiming for specific improvements as compared to the ITER divertor:

- Utilising the divertor heat for electricity production at acceptable efficiency would require a coolant temperature of > 250 °C.
- The material Cu:Cr:Zr used on ITER should be replaced by a material which has low activation properties, in order to minimise the amount of radioactive waste with longer decay times.

On top of the stationary loads, edge localised modes (ELMs) associated with the standard H-mode would provide strong pulsed heat loads to the divertor surface. Uncontrolled ELMs would deposit energies of several 10 MJ per ELM on ITER, and up to 100 MJ per ELM on DEMO [28], which would lead to surface melting if no mitigation measures are taken. While ITER is aiming to mitigate ELMs by employing resonant magnetic pertubations and ELM pacing via Pellet injection, the

required ELM mitigation factor for DEMO and the requirements for reliability of ELM suppression are so high that a change in the dis-charge scenario, i. e. an intrinsically ELM-free discharge type, appears favourable.

The power exhaust problem explained above is currently seen as the most important issue where substantial progress will be needed in order to make commercial fusion viable, and intense R&D is being pursued to develop solutions. In the current stage of fusion research, Tungsten is widely regarded as the prime choice for first wall and divertor surface materials, since it first provides high resilience against erosion by physical sputtering due to its high atomic mass, second high resilience against stationary and transient heat loads due to the good thermal conductivity and the high melting point, and third it shows acceptable levels of activation after neutron irradiation. In the current EU DEMO development it is therefore seen as the baseline solution for both the first wall as well as the divertor material.

However, even when assuming that the power flow across the separatrix is being reduced via core plasma radiation down towards the H mode threshold, $P_{SOL} \sim P_{LH}$, the remaining power flux density towards the divertor target plates may be still too high. To solve this problem, three main alternative approaches to the baseline divertor are being pursued: First, divertor strike point sweeping with an amplitude of several 10 cm and a frequency in the order of 1 Hz is being explored as an option to distribute the power fluxes over a larger part of the divertor target. Second, novel magnetic configurations are being investigated, aiming to reduce the power flux densities to the divertor by a magnetic field structure which is spreading the field lines from the edge plasma onto larger parts of the divertor target. Third, parts of the divertor surface could be made of liquid metal which is flowing and thereby enhancing the heat removal due to its heat capacity. None of these concepts has reached sufficient maturity until now, so that these are not foreseen in the current ITER design.

IV. DESIGN OPTIMISATION OF A TOKAMAK FUSION REACTOR

Having summarised the main physics and technological constraints for tokamak fusion reactor design, we can now proceed discussing the tokamak fusion reactor equation (20) and suitable optimisation criteria. In order to better show the explicit dependencies on technical quantities that can be independently chosen, we substitute eq. (33) into eq. (20). Moreover, considering also the case of plasma dilution by impurities, we use $f_{nDT} = n_{DT}/n_e$ and $s_{nz} = \sum n_z/n_e$ and obtain a more detailed version of the tokamak fusion reactor equation

$$P_{\alpha,M} = 0.004\, H_H^{5.26} a^{7.58} R_0^{-2.37} \kappa^{1.47} f^{7.05} \times N_{GW}^{2.16} \left(\frac{f_{nDT}}{1 + f_{nDT} + s_{nz}} \right)^{5.26} q_{95}^{-7.05} B_{\max}^{7.84} \left(1 - \frac{a+b}{R_0} \right)^{7.84} . \quad (35)$$

We note that there is still the dependence of the shape factor f from the elongation, triangularity and aspect ratio, see eq. (10). Furthermore, the maximum controllable elongation depends on the aspect ratio according to eq. (11). However, in order to keep the reactor equation reasonable simple, we will not substitute these further.

Equation (35) can now be used to discuss the recipe for optimisation of a tokamak fusion reactor. In general, for a reactor ultimately the cost of electricity (*CoE*) should be minimised, which means maximisation of the net electrical output power while minimising the overall reactor cost for initial investment, operation, maintenance, shutdown and disposal. The presentation of a full fusion reactor cost model is beyond the scope of the present paper. However, as a first approximation, we may assume that the cost of electricity is proportional to the total volume of the tokamak components (blanket, vessel, coils, etc.), hence

$$CoE \sim \frac{V_{tokamak}}{P_{el.,net}} \quad (36)$$

In further determining the optimum choice of parameters in eq. (35), the maximisation of many individual parameters may be desirable but a number of operational and technical limits have to be obeyed:

- The TF coil system should be optimised for the maximum technically possible magnetic field B_{max}, which amounts ~ 12 ... 13 T according to current technology as described above.
- The radial build should be optimised for minimum blanket thickness, hence $b \sim 1.8$ m.
- The maximum possible plasma current compatible with good MHD stability should be chosen, yielding $q_{95} \sim 3$.
- A high plasma density should be chosen, which is favourable for both high fusion power but also for power exhaust (detached divertor). This means operation near the Greenwald limit with $N_{GW} \sim 1$, noting that this density limit is related to the edge plasma density, so that in case of peaked density profiles a mean density of $N_{GW} \sim 1$ is viable.
- The elongation should be chosen such that a reliable control of the vertical plasma position is possible: $\kappa \sim 1.6 ... 1.8$. On the same time, the triangularity should be maximised with respect to the limits of what is achievable based on the feasibility and cost of PF coils.
- A stable plasma scenario should be chosen with high core radiation but observing the requirement of $P_{loss} > P_{LH}$. We note that for highly radiative H-mode usually $H_H <= 1$ is found [29,30]. On the other hand, since the confinement scaling (eq. 6) was elaborated while neglecting the radiation correction assuming $P_{loss} = P_{heat}$, an effective confinement quality of $H_H = 1.0$ may be seen as viable for DEMO [31].

Making use of these boundary conditions in a consistent fashion, only two open parameters are left, namely the

major plasma radius R_0 and aspect ratio $A = R_0 / a$, which can now be selected independently to choose the target fusion power and pulse duration of the tokamak reactor.

V. SELECTED NUMERICAL RESULTS

In the following, we present selected numerical results derived from the reactor systems model described above, where profile effects have been included. In figure 2 the cost of electricity is displayed using a conservative set of input parameters H_H = 1.0, N_{GW} = 1.0, q_{95} = 3, P_{ext} = 50 MW, $B_{max,TF} = B_{max,CS}$ = 13 T, b = 1.8 m, while for the elongation eq. (11) was used and for the triangularity $\delta = (\kappa - 1)/2$ was assumed. The range of plotted data covers the range in which numerical solutions were found in agreement with the chosen input data and with a power flow across the separatrix $P_{sep} > P_{LH}$.

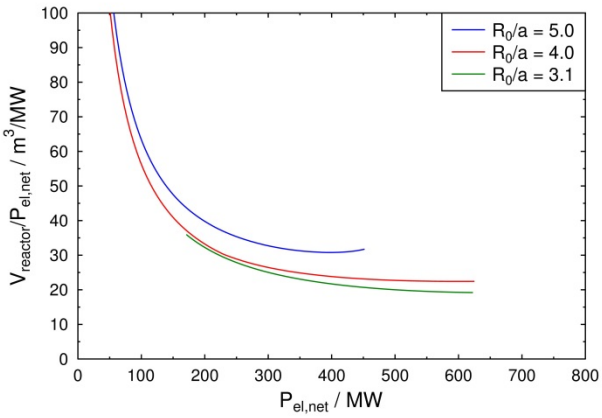

Figure 2: Cost of electricity for different aspect ratios

This simplified cost of electricity figure typically shows a steep decrease with increasing electrical output power (reactor size), up to a point of saturation at a few 100 MW from which onwards a further increase of the reactor size does not lead to further improvement. The main reasons for this observed saturation are:

- Increasing the machine size leads to an increase of plasma temperature. However, for plasma temperatures of $T > 20$ keV the fusion rate coefficient shows only a moderate increase, with saturation above $T >$ 40 keV, see fig. 1.
- With increasing major radius R_0, the absolute achievable plasma density due to the Greenwald limit decreases, which becomes evident when inserting eq. (9) in eq. (8). On the same time however, the magnetic field in the plasma B_0 can be increased according to eq. (33), if B_{max} is kept constant.
- With increasing fusion power and reactor size a larger fraction of the power has to be radiated in order to keep the divertor load below the limits. This is accomplished via impurity seeding, causing additional plasma cooling and some dilution of the fuel, both reducing the further increase in fusion power.

Based on the results of fig. 2 we may conclude that the optimisation of cost of electricity leads us towards a minimum plant size in the order of several 100 MW electrical output power. This refers to a typical minor plasma radius of $a \sim 2.5 \ldots 2.8$ m, i.e. a reactor size about 25…40 percent larger than ITER.

The pulse duration for the same cases is displayed in figure 3. We note that for large aspect ratio the achievable pulse duration can be substantially longer than for small aspect ratio. The main reason is that with the larger R_0 more space is available in the centre of the tokamak, which allows installing a larger CS coil which can provide a larger total flux Φ_0.

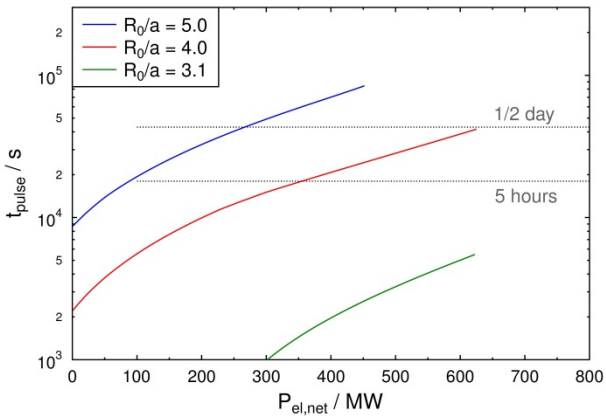

Figure 3: Pulse duration for different aspect ratios

The numerical examples presented above demonstrate that the two main dimensional parameters a and R_0 are suitable parameters to define the tokamak geometry based on target values for electrical output power and pulse duration, after having defined all other parameters from eq. (35) according to operational and technical limits.

Defining several technical and physics parameters near their limits, namely elongation, triangularity, plasma density and safety factor, we can see that in eq. (35) the fusion power depends on the product of high powers of confinement quality H_H, magnetic field B_{max} and reactor dimensions. We may conclude that, for a defined target fusion power, a reduction of the size of the tokamak (minor and major radius) could be achieved if a higher magnetic field $B_{max} > 13$ T or a better plasma confinement $H_H > 1$ could be obtained as compared to the status of today's fusion research. Improving the plasma confinement and designing stronger magnetic field coils are therefore subjects of ongoing research. However, a more compact tokamak with high fusion power would have to solve the even stronger power exhaust problems arising from the higher power densities.

VI. THE STELLARATOR: AN ALTERNATIVE CONFINEMENT CONCEPT

Instead of driving a current in the plasma, the necessary helical structure of the confining magnetic field in a

toroidal system can be fully defined by external magnetic field coils. This is the approach of the stellarator, with the largest currently existing devices being the Heliotron type device LHD [32] and the optimised stellarator W7-X [33,34]. Important intrinsic advantages of the stellarator are [34] first the possibility of steady state plasma operation without the need to maintain a plasma current, second the fact that the confining field structure is fully determined from outside, so that plasma instabilities cannot lead to an as sudden loss of confinement like in a tokamak. On the other hand, the externally defined helical field structure is associated with a non-axisymmetric complex geometry of field lines, with a large fraction of trapped plasma particles, and causing significant challenges for the machine design and engineering. While the drift losses of trapped particles from the complex confining field structure can be reduced by the optimised field structure [33, 34], the engineering issues towards a future stellarator reactor design remain challenging [35] in particular with respect to coil geometry and magnetic forces, as well as the overall maintenance concept.

Within the European fusion research, the development of the stellarator is being pursued as a promising alternative to the tokamak and may become the candidate approach for a DEMO fusion reactor after successful operation of W7-X.

VII. SUMMARY

Within this paper, we have summarised the status and prospects of the development towards a tokamak fusion reactor. For this purpose, a numerical model was proposed which describes the main features of the tokamak reactor based on a limited number of input parameters. Defining the values for a number of plasma physics and technological quantities nearby the known limits, the main dimensions of the tokamak, a and R_0, remain as optimisation quantities, from which the net electrical output power and the pulse duration of the tokamak can be derived in a straight-forward manner.

REFERENCES

[1] www.iter.org

[2[Romanelli F. et al., Fusion electricity, https://www.euro-fusion.org/wpcms/wp-content/uploads/2013/01/JG12.356-web.pdf (2012)

[3] Wagner F. et al., Plasma Phys. Control. Fusion **52** (2010) 124044

[4] Wesson J., Tokamaks, Oxford Univ. Press, 4th Edition (2011)

[5] Bosch H. S. et al., Nucl. Fusion **32** (1992) 611

[6] Wagner F., Plasma Phys. Control. Fusion **49** (2007) B1

[7] ITER Physics Expert Group on Confinement and Transport et al., Nucl. Fusion **39** (1999) 2175

[8] Martin Y. R. et al., J. of Physics: Conf. Series **123** (2008) 012033

[9] Koslowski H. R., these proceedings (2015)

[10] Greenwald M., Plasma Phys. Control. Fusion **44** (2002) R27

[11] ITER Physics Expert Group on Disruptions, Plasma Control, and MHD and ITER Physics Basis Editors, Nucl. Fusion **39** (1999) 2251

[12] Zohm H. et al, Nucl. Fusion **53** (2013) 073019

[13] Kovari M. et al., Fusion Engin. Design **89** (2014) 3054

[14] Johner J., Fusion Sci. Technol. **59** (2011) 308

[15] Dragojlovic Z. et al., Fusion Engin. Design **85** (2010) 243

[16] Zohm H., Fusion Sci. Technol. **58** (2010) 613

[17] Kallenbach A. et al., Nucl. Fusion **52** (2012) 122003

[18] Matthews G. F. et al., J. Nucl. Materials **241-243** (1999) 450

[19] Sheffield J., Rev. Mod. Phys. **66** (1994) 1015

[20] Ejima S. et al. Nucl. Fusion **22** (1982) 1313

[21] Wolf R. C., Plasma Phys. Control. Fusion **45** (2003) R1

[22] Mitchell N. et al., Fusion Engin. Design **84** (2009) 113

[23] Duchateau J.-L. et al., Fusion Engin. Design **89** (2014) 2606

[24] Zeng S. and Todd T., Fusion Engin. Design, in press (2015)

[25] Boccaccini L., Fusion Sci. Technol. **64** (2013) 615

[26] Lehnen M. et al., J. Nucl. Materials **463** (2015) 39

[27] Hirai T. et al., Fusion Engin. Design **82** (2007) 389

[28] Wenninger R. et al., Nucl. Fusion **54** (2014) 114003

[29] Rapp J. et al., Nucl. Fusion **49** (2009) 095012

[30] Asakura N. et al., Nucl. Fusion **49** (2009) 115010

[31] Ward D. J., Plasma Phys. Control. Fusion **52** (2010) 124033

[32] Iiyoshi, A., et al., Fusion Technol. **17** (1990) 169

[33] Gasparotto M. et al., Fusion Engin. Design **89** (2014) 2121

[34] Helander P. et al., Plasma Phys. Control. Fusion **54** (2012) 124009

[35] Schauer F. et al., Fusion Engin. Design **88** (2013) 1619